PNAS
www.pnas.org

Supplementary Information for

Intraluminal pressure elevates intracellular calcium and contracts CNS pericytes: Role of voltage-dependent calcium channels.

Nicholas R. Klug, Maria Sancho, Albert L. Gonzales, Thomas J. Heppner, Rochelle Irene C. O'Brien, David Hill-Eubanks, Mark T. Nelson

Nicholas R. Klug,

Email: nicholas.klug@uvm.edu

and

Mark T. Nelson,

Email: mark.nelson@uvm.edu

This PDF file includes:

Supplementary methods text

Figures S1 to S5

Supplement references

Supplementary Information Text

Supplementary Methods

Animals

All animals were used in accordance with protocols approved by the Institutional Animal Care and Use Committee of the University of Vermont. Adult (2–6-month-old) male mice were euthanized by intraperitoneal (i.p.) injection of sodium pentobarbital (100 mg/kg) and subsequent rapid decapitation. Animals were group-housed on a 12-hour light/dark cycle with environmental enrichment and free access to food and water. The following mice strains were used: C57BL/6J (stock no. 000604; Jackson Laboratories), NG2-DSRed (stock no. 008241), and Ai95 (RCL-GCaMP6f) mice (stock no. 028865; Jackson Laboratories) expressing the genetically encoded Ca^{2+} indicator GCaMP6f. These latter mice were crossed with Myh11-Cre^{ERT2} mice (courtesy of Dr. Stefan Offermanns (1)) to generate Myh11-GCaMP6f mice, in which GCaMP6f expression is driven by tamoxifen-inducible Cre recombinase under control of the myosin heavy chain 11 (*Myh11*) promoter. Tamoxifen citrate food (cat. No. TD.130859; Envigo) was administered to 9–12-week-old Myh11-GCaMP6f mice for seven consecutive days.

Pressurized *ex vivo* retina preparation

After euthanizing mice, the overlying skull and brain were carefully removed, after which the eye, surrounding orbit bones, connected musculature, vasculature, and optic nerve were removed in one piece using angled eye scissors and placed in 4°C Ca^{2+}-free retina dissection buffer (119 mM NaCl, 3 mM KCl, 0 mM $CaCl_2$, 3 mM $MgCl_2$, 5 mM glucose, 26.2 mM $NaHCO_3$, 1 mM NaH_2PO_4, bubbled with 95% O_2/5% CO_2, pH 7.4). The surrounding bones and outer muscles were removed into a 4°C dissection dish with intermittent exchange of bubbled dissection solution, and the inner muscles and connective tissue were removed, revealing the ophthalmic artery, which enters the retina at the base of the optic nerve. The cornea was pierced using fine forceps, and the entire cornea and iris were removed using a circumferential cut. The lens was grasped with fine forceps, after which the connective tissue of the ora searrata was disrupted and the lens was removed using closed, semi-fine, blunt forceps. Fine dissection scissors were used to remove the sclera, leaving a patch of scleral tissue around the base of the optic nerve.

Using a large barrel transfer pipette, the dissected retina was transferred to a custom myography chamber containing room temperature retina dissection buffer. The ophthalmic artery was then cannulated

using a pulled borosilicate glass pipette (~100–150 µm tip diameter) filled with retina physiological salt solution (rPSS; 119 mM NaCl, 3 mM KCl, 2 mM $CaCl_2$, 1 mM $MgCl_2$, 5 mM glucose, 26.2 mM $NaHCO_3$, 1 mM NaH_2PO_4), maintained at pH 7.4 by bubbling with 95% O2/5% CO_2. Loose ophthalmic artery branches were tied off using a monofilament nylon fiber (cat. THR-G; Living Systems), and the cannulated vessel was secured to the pipette. The tip of the cannulation pipette was advanced in such a manner that the downstream ophthalmic artery was narrower than the tip of the pipette, a maneuver that allows the remaining ophthalmic artery and retinal artery vasculature rather than the tip of the pipette to set inlet flow. The retina was placed over a custom silicone platform and flattened by making radial cuts in the outer edges, after which the retina was secured to the platform using short pins cut from a 70-µm diameter tungsten wire (Figure 2). The cannulation pipette was attached to a pressure transducer to allow measurement of pressure at the level of the ophthalmic artery and connected to two solution columns, linked via a 3-way adjustable valve. One column was fixed at a height providing a pressure of 20 mmHg and the other was adjustable, providing a full range of pressures from 0 to 100 mmHg. This allowed for sustained pressure steps by incrementally changing the adjustable column height. Successful retinal vessel canulation was confirmed by pressurizing the retina to 60 mmHg and monitoring rapid removal of blood cells from the vasculature via brightfield microscopy. Bath perfusion (with bubbled rPSS) was kept constant at 5 mL/min (3 mL/min for microelectrode experiments), and a temperature of 35–36°C was maintained using an inline heater. The preparation was allowed to equilibrate for 20 minutes at 60 mmHg before the start of experimentation.

Immunohistochemistry

Following euthanasia, eyes were enucleated and placed in 4% paraformaldehyde, diluted in phosphate-buffered saline (PBS), for 2 hours at 4°C. Whole retinas were dissected from eyes and blocked and permeabilized by incubating with PBS containing 5% bovine serum albumin (BSA) and 0.2% Triton X-100 at room temperature for 2 hours. Retinas were then incubated for 24 hours with primary antibody (and/or conjugated hydrazide), diluted in PBS containing 0.5% BSA and 0.2% Triton X-100 at 4°C. The following conjugated antibodies/stains were used at the indicated dilutions: Cy3-conjugated anti-αSMA (1:2000, cat. no. C6198; Sigma), fluorescein isothiocyanate (FITC)-conjugated anti-αSMA (1:2000, cat. No. F3777; Sigma), and 633-hydrazide (1:1000 from 1.2 mM stock, cat. No. 92156; Biotium). Retinas were washed three times in PBS for 10 minutes each at room temperature, after which radial slits were made to create a flat-

mount preparation, which was then placed under coverslips and stabilized using Vectashield Plus mounting media (Vector Laboratories). For acquisition of GCaMP (GFP) fluorescence, live dissected retinas were first placed into 120 mM K^+ rPSS, with equimolar subtraction of NaCl, for 5 minutes to depolarize mural cells and increase detectable GCaMP fluorescence and then fixed in 4% paraformaldehyde. Images were acquired with an upright 10X air (0.1 NA) or 16X water-immersion (0.8 NA) objective utilizing widefield or multiphoton microscopy (Scientifica Hyperscope; United Kingdom).

Vessel diameter and Ca^{2+} imaging

Retinal vessels of C57BL/6J mice were visualized by staining with FITC-conjugated isolectin B4 (Bandeiraea simplicifolia, cat. no. ALX-650-001F-MC0; Enzo Life Sciences, Inc.), here referred to simply as lectin, which binds to α-galactosyl residues of the vascular glycocalyx (2). For lectin application, bath perfusion was stopped and 10 μL of FITC-conjugated lectin (stock concentration, 0.5 mg/mL) was pipetted directly onto the retina (bath volume, ~2.5 mL) and incubated for 10 minutes. Following lectin application, bath perfusion with rPSS was maintained for 20 minutes before experimentation. Pressure in lectin-stained vessels was increased and sustained as described in each experimental series. The pressure-specific passive diameter was achieved by bath-perfusing for 10 minutes with EGTA-containing Ca^{2+}-free buffer (119 mM NaCl, 3 mM KCl, 0 mM $CaCl_2$, 1 mM $MgCl_2$, 5 mM glucose, 26.2 mM $NaHCO_3$, 1 mM NaH_2PO_4, 5 mM EGTA), maintained at pH 7.4 by bubbling with 95% O_2/5% CO_2. After measurement of active diameters (in buffer containing 2 mM external Ca^{2+}) and passive diameters (in buffer containing 0 mM external Ca^{2+}), arterioles were distinguished from capillary branches by staining the IEL with Texas Red-conjugated hydrazide (40 μM, cat. No. 481; AAT Bioquest), added to the cannulation solution. A bypass outlet located near the cannula was then opened to purge non-fluorescent cannula solution, after which the entire retina was perfused with cannula solution containing Texas Red hydrazide for 10 minutes. The hydrazide-containing solution was purged via the bypass outlet, and rPSS was perfused for an additional 10 minutes, resulting in prominent red staining of the arteriolar IEL. Abluminal diameters and IEL staining were measured in serial z-stack images (collected using ~0.7 full-vessel–depth z-stacks/s at a frame rate of 13 Hz [for all rapid serial z-stack imaging]) obtained at each pressure step.

Constriction of vessels in 2 mM external Ca^{2+} (active diameter) was calculated relative to that of passive diameters in 0 mM external Ca^{2+} as a percentage, as follows:

% Constriction at each pressure step = (passive diameter – active diameter)/passive diameter × 100.

Nifedipine-specific dilation was similarly calculated as follows:

% Nifedipine-specific dilation = ([{nifedipine diameter – baseline 80 mmHg diameter} – {0 mM external Ca^{2+} diameter – baseline 80 mmHg diameter}]/[0 mM external Ca^{2+} diameter – baseline 80 mmHg diameter]) × 100.

Intracellular Ca^{2+} measurements

GCaMP6f fluorescence intensity was used as an indicator of cytosolic Ca^{2+} levels, where an increase in fluorescence intensity corresponds to an increase in cytosolic Ca^{2+} concentration. Changes in GCaMP6f fluorescence were imaged using a Revolution spinning-disk confocal microscope system equipped with two iXon Life 16-bit EMCCD cameras (Andor Technology) attached to a Nikon microscope. Either 60X (numerical aperture [NA] 1.0) or 40X (NA 0.8) objectives were used, and fluorescence was excited using a 488-nm or 560-nm solid-state laser. Emitted fluorescence was collected through a 527.5/49 nm or 641.5/117 nm band-pass filter.

Pressure changes and vascular responses in the whole retina preparation caused considerable z-drift and alterations in vessel area during single-plane fluorescence imaging, a factor that precludes the use of the commonly applied fractional fluorescence change ($\Delta F/F_0$) quantitation approach. To account for movement in the z-plane, we employed a time-averaged, whole-vessel fluorescent value—an indicator of whole-cell cytosolic Ca^{2+} levels. This was achieved by repeatedly imaging through the entire depth of vessels at a frame rate of ~13 frames/s while continuously moving through the entire z-plane of all superficial vessels. Approximately 22 full z-sweeps were achieved in a 30-second imaging window (~0.7 z-stacks/s). Frame-by-frame maximal fluorescence values were projected into a single fluorescent image, reflecting the peak fluorescence value per pixel during the 30-second imaging period. The final z-projection of fluorescence values was used to generate fluorescence intensity values for SMCs and pericytes.

A single fluorescence value (16-bit scale) for SMCs or pericytes at a particular branch order (vascular segment) was generated by drawing 3–5 (depending on vessel length) evenly spaced, perpendicular regions of interest (ROIs; 4-μm–width lines) and averaging individual ROI fluorescence values from vessel cross sections. Image analysis was completed using ImageJ software. Percent change in fluorescence was calculated according to the following formula:

% Change = ([80 mmHg fluorescence value – 20 mmHg fluorescence value]/[20 mmHg fluorescence value]) × 100.

Fluorescent bead imaging

Intraluminal flow velocity in the intact pressurized retina vasculature was visualized using fluorescent beads and a widefield fluorescence microscope (Olympus MVX 10) equipped with a sCMOS camera (Andor Zyla 4.2). Plasma flow properties were assessed by adding 1-μm diameter fluorescent polystyrene beads (cat. F13081; Invitrogen) to the pressure column solution. Intermittent single-sphere flow trajectories were achieved by diluting beads (stock, 2% solids; sonicated) 1:200 in fetal bovine serum. Diluted beads were allowed to stand at RT for 30 minutes in the presence of serum proteins. Beads in fetal bovine serum were further diluted 1:1,500 into the pressure column solution.

Whole retina widefield imaging in wild-type tissue (non-fluorescent vasculature) allowed for accurate diameter measurements of venules, providing an aggregate flow measurement for all vessels with intact flow (i.e., all but the very few cut vessels that do not drain into venules). Changes in venule flow are directly proportional to perfusion changes throughout the whole tissue (3, 4) and are calculated as flow = vessel area × velocity, where area = πr^2. Velocity values were generated from frame-by-frame distance/time measurements, averaged within single vessels.

Electrophysiology

Membrane potential measurement

Membrane potential in intact pressurized retinal vascular cells was measured as previously reported (5). After equilibration of the pressurized preparation, perfusion was stopped and superficial connective tissue was mildly enzymatically digested by layering 170–200 μL of papain solution (2 U/mL in rPSS; Worthington) directly onto the retina preparation (bath volume, ~2.5 mL) to improve microelectrode impalement. After allowing to stand for 3 minutes, papain was washed away by bath perfusion, and the preparation was allowed to equilibrate for an additional 10–20 minutes. Superficial pericytes within the transition zone or at more distal locations in the capillary bed, identifiable by their prominent bump-on-a-log perivascular morphology, were located using brightfield microscopy. Borosilicate microelectrodes, pulled to a resistance of ~200–300 MΩ, were filled with a 0.5 M KCl solution containing 3 μM iFluor 488 hydrazide (AAT Bioquest). Cells were impaled, and membrane potential was recorded using an AxoClamp-2A digital amplifier and HS-2

headstage (Molecular Devices) and digitized using Digidata 1322A and PClamp 9 software (Molecular Devices). Criteria for a successful recording included 1) a sudden negative membrane potential at the time of impalement; 2) relatively steady membrane potential values for at least 1 minute (with allowance for commonplace oscillations); and 3) sudden return of membrane potential to 0 mV following removal of the microelectrode. Pericyte impalement and branch order were verified by imaging 488-hydrazide–filled cells and Texas Red hydrazide-stained IEL using spinning-disk confocal microscopy.

Patch-clamp technique

Pericytes were isolated from NG2-DsRed mouse brains and eyes by mechanical disruption of a small piece of brain somatosensory cortex or both mouse retinas (volume, ~10–20 mm^3) using a papain-based Neural Tissue Dissociation kit (Miltenyi Biotec), as previously described (5-7). Briefly, tissue was cut into very small pieces with sharp scissors, transferred to ice-cold dissociation solution (10 mM HEPES pH 7.3, 55 mM NaCl, 80 mM Na-glutamate, 5.6 mM KCl, 2 mM $MgCl_2$, 4 mM glucose) containing enzyme 1 (provide in the kit), and incubated for 17 minutes at 37°C. Enzyme 2 was then added and the solution was mixed 10 times using a Pasteur pipette. After incubating for 12 minutes at 37°C, the brain suspension was passed 10 times through a 20 G needle and incubated for an additional 10 minutes at 37°C. The cell suspension was then filtered through a 62-μm nylon mesh and stored in ice-cold dissociation solution. Freshly isolated cells were used the same day (within ~5 hours).

Single SMCs were isolated from cerebral pial arteries and arterioles from C57BL/6J mice. Following dissection, artery and arteriole segments were stored in ice-cold dissociation solution. SMCs were enzymatically dissociated by placing artery and arteriole segments in dissociation solution containing 0.3 mg/ml papain (Worthington) and 0.3 mg/ml dithioerythritol (Sigma) for 14 minutes at 37°C. Segments were then washed with dissociation solution and placed in dissociation solution containing 0.67 mg/ml collagenase F, 0.33 mg/ml collagenase H (Sigma), and 100 μM $CaCl_2$ for 5 minutes at 37°C. After washing vessels with dissociation solution, single SMCs were released by trituration with a fire-polished glass Pasteur pipette and stored in ice-cold dissection medium for same day use (~5 hours).

Ca^{2+} currents in isolated pericytes and SMCs were measured in the conventional whole-cell configuration of the patch-clamp technique. Currents were amplified using an Axopatch 200 amplifier, filtered at 1 kHz, digitized at 10 kHz, and stored on a computer for offline analysis with Clampfit 10.7

software (Molecular Devices). Whole-cell capacitance and series access resistance were measured using the cancellation circuity in the voltage-clamp amplifier. Patch pipettes were pulled from borosilicate glass microcapillary tubes (1.5 mm OD, 1.17 mm ID; Shutter Instruments) and fire-polished (resistance, 3–5 MΩ). Cells were voltage clamped and equilibrated in external (bathing) solution containing 10 mM HEPES (pH 7.4), 10 mM NaCl, 1 mM CsCl, 10 mM $BaCl_2$, 1.2 mM $MgCl_2$, 10 mM glucose. The pipette (internal) solution contained 10 mM HEPES, 135 mM CsCl, 5 mM Mg-ATP, and 10 mM EGTA (pH 7.2, adjusted with CsOH). The L-type Ca^{2+} channel activator Bay K 8644 (500 nM; Tocris) was included in the bathing solution to promote long-lasting openings (8). Whole-cell currents were recorded from isolated pericytes and SMCs voltage clamped at a holding potential of -60 mV and subjected to a -90 mV prepulse (200 ms) followed by a +10 mV voltage step (300 ms). The mean capacitance of retinal pericytes averaged 10.7 ± 0.6 pF (n = 6); the mean capacitance of brain pericytes averaged 10.0 ± 0.5 pF (n = 6); and the mean capacitance of brain pial SMCs averaged 13.4 ± 0.6 pF (n = 12). All experiments were performed at room temperature (~22°C).

Supplementary Figures

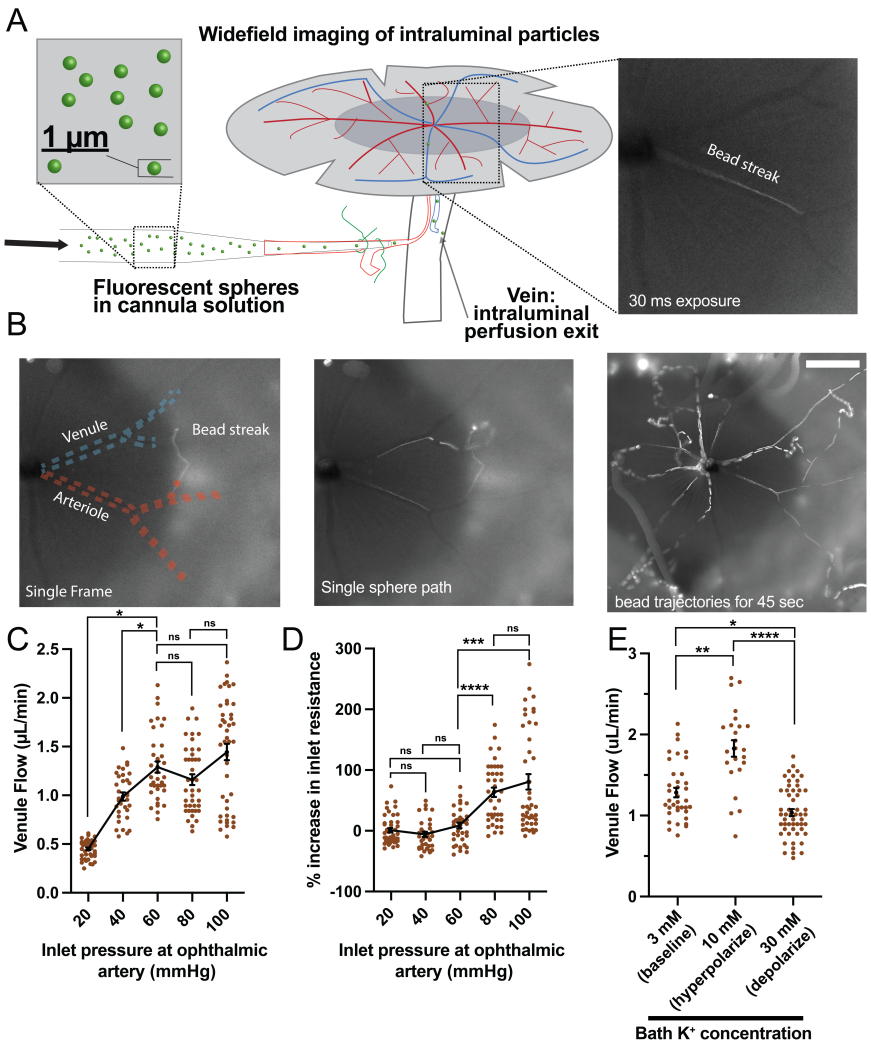

Supplemental Figure 1: Intraluminal fluorescent particles provide specific flow and patterning information. **A.** Fluorescent beads added to the cannulation solution and imaged using fluorescence widefield microscopy. Rapid imaging (<30 ms exposure) provides zone-specific velocity information; example presented here shows distance bead traveled in a retinal arteriole in 30 ms. **B.** Bead path, determined through continuous rapid imaging, where multiple bead trajectories consist of many individual bead paths averaged over time (45 seconds in this example). Scale bar: 500 µm. **C.** Flow in the retinal venule at intraluminal pressures of 20–100 mmHg. **D.** Network resistance values at pressures of 20–100 mmHg, generated using data from C. **E.** Flow in the retinal venule at 60 mmHg with isotonic bath K^+ concentrations of 3, 10, and 30 mM. Data are presented as individual values and means ± SEM (*p < 0.05, **p < 0.01, ***p < 0.001, ****p < 0.0001, Kruskal-Wallis test with Dunn's multiple comparison test); ns, not significant. Data are from n = 3 retina preparations with confirmed arteriolar tone (arterioles initially imaged at higher magnification).

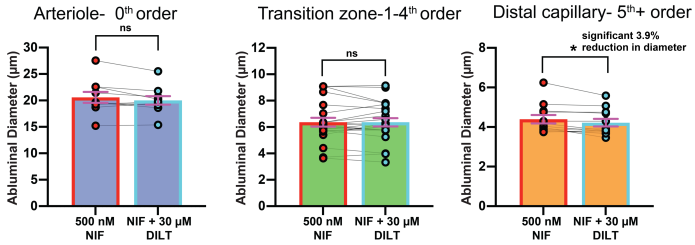

Supplemental Figure 2: Changes in vessel abluminal diameter under nifedipine only and nifedipine plus diltiazem conditions. Abluminal diameters of arterioles and capillaries (with confirmed development of constriction at 80 mmHg intraluminal pressure) following bath application of 500 nM nifedipine and subsequent application of 30 µM diltiazem. Data are paired individual values ± SEM (n per zone = 8–22 from 3 animals; *p < 0.05, paired t-test); ns, not significant.

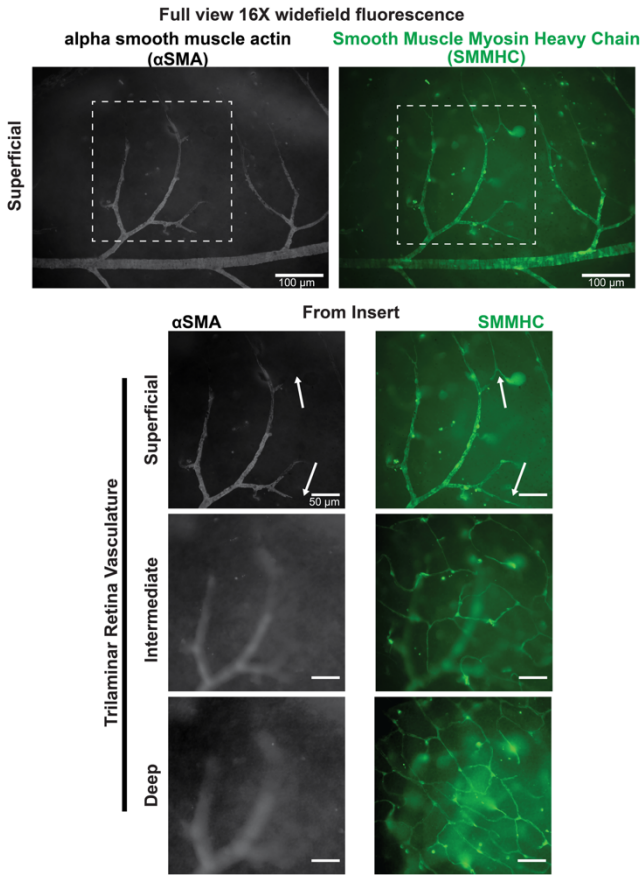

Supplemental Figure 3: *myh11*-driven GCaMP6f and αSMA expression in the retinal vasculature. **A.** Retinas from *myh11*-GCaMP6f mice, fixed and stained for αSMA. Widefield images show distinct αSMA staining in arterioles and transition zone branches. Endogenous, fixed GCaMP fluorescence illuminates arterioles and transition zone branches. GCaMP fluorescence also extends to all pericytes covering transition zone and distal capillaries throughout the trilaminar vascular network of the retina. Arrows show capillary branches lacking αSMA and continuation of GCaMP6f expression. Scale bars, 50 µm.

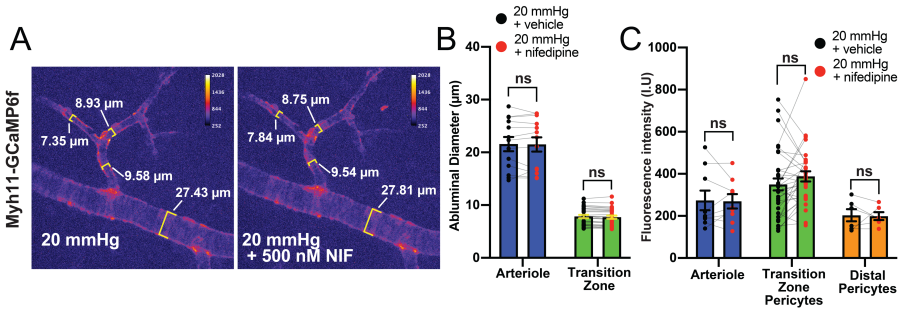

Supplemental Figure 4: Voltage-dependent changes in cytosolic Ca^{2+} in pericytes. **A–C.** Arteriolar and transition zone capillary diameters and cytosolic Ca^{2+} (GCaMP6f fluorescence), with and without 500 nM nifedipine (NIF), measured at low pressure (20 mmHg) in a retinal preparation from an *Myh11*-GCaMP6f mouse. **A**. Representative pseudocolored image of GCaMP6f fluorescence, with vascular diameters indicated. Distal diameters could not be measured using abluminal GCaMP coverage due to non-continuous abluminal coverage by string projections. **B**. Summary data showing arteriole and transition zone capillary diameters. Abluminal diameter determined using GCaMP6f fluorescence; distal capillary diameters were not calculated due to incomplete abluminal coverage of distal thin strand pericytes (lectin not used) **C.** Summary data showing Ca^{2+} levels (GCaMP6f fluorescence values) in arterioles and capillaries (transition zone and distal). Data are paired individual values presented with means ± SEM (n = 6–32 vessels from 5–7 animals; *p < 0.05, paired t-test); ns, not significant.

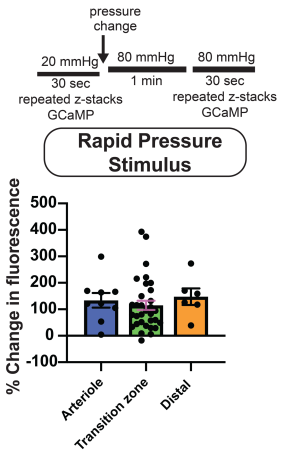

Supplemental Figure 5: Schematic of protocol to measure Ca^{2+} 1 minute after pressure elevation. Pressure-induced (20 to 80 mmHg at ophthalmic artery) changes in Ca^{2+} (GCaMP6f fluorescence) in arterioles, transition zone capillaries, and distal capillaries 1 minute after pressure elevation. Data are individual values presented with means ± SEM (n = 6–32 vessel segments from N = 5–10 animals).

Supplement References

1. A. Wirth *et al.*, G12-G13-LARG-mediated signaling in vascular smooth muscle is required for salt-induced hypertension. *Nat Med* **14**, 64-68 (2008).
2. B. P. Peters, I. J. Goldstein, The use of fluorescein-conjugated Bandeiraea simplicifolia B4-isolectin as a histochemical reagent for the detection of alpha-D-galactopyranosyl groups. Their occurrence in basement membranes. *Exp Cell Res* **120**, 321-334 (1979).
3. G. T. Feke *et al.*, Blood flow in the normal human retina. *Invest Ophthalmol Vis Sci* **30**, 58-65 (1989).
4. V. Patel, S. Rassam, R. Newsom, J. Wiek, E. Kohner, Retinal blood flow in diabetic retinopathy. *BMJ* **305**, 678-683 (1992).
5. M. Sancho *et al.*, Adenosine signaling activates ATP-sensitive K(+) channels in endothelial cells and pericytes in CNS capillaries. *Sci Signal* **15**, eabl5405 (2022).
6. L. He *et al.*, Single-cell RNA sequencing of mouse brain and lung vascular and vessel-associated cell types. *Sci Data* **5**, 180160 (2018).
7. M. Vanlandewijck *et al.*, A molecular atlas of cell types and zonation in the brain vasculature. *Nature* **554**, 475-480 (2018).
8. J. M. Quayle, J. G. McCarron, J. R. Asbury, M. T. Nelson, Single calcium channels in resistance-sized cerebral arteries from rats. *Am J Physiol* **264**, H470-478 (1993).